lyotropic liquid crystal (LLC) made from lipid, MPC polymer and Nafion membrane as an overcoating membrane. Nafion dispersion solution was purchased from Wako, 2-Methacryloyloxythyl phosphorylcholine (MPC) polymer was purchased from NOF Corporation, and LLC was made from 1-oleoyl-rac-glycerol as reported procedure [6]. Each surface modification was conducted 30 min before the measurements.

Biocompatibilities of the polymer-coated electrodes were judged from amount of adsorbed protein. Each electrode was soaked in a PBS solution of fluorescence-labeled albumin (Albumin, Fluorescein isothiocyanate conjugate bovine serum, SIGMA) for 1, 3, 6, 12 hours and washed with buffer solution before measurements. Fluorescent micrographs were recorded using the LAS-3000mini, a compact Luminescent Image analyzer (Fuji film). Exposure times were 10 s. The images were analyzed using Multi Gauge software (version 3.0, Fuji film).

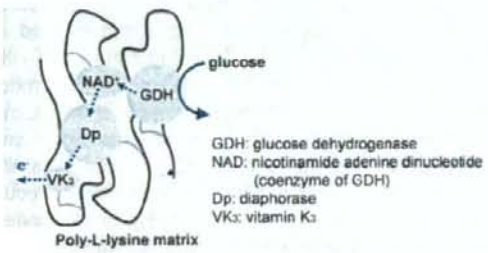

Fig. 2: Schematic of electron relay at the bioanode

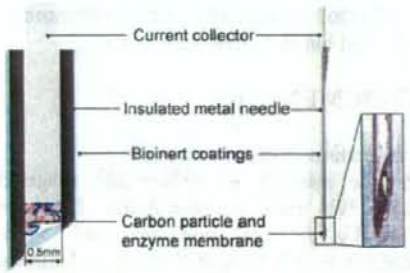

Fig. 3: Schematic illustration (left) and photograph (right) of the prototype of needle-type biofuel cell.

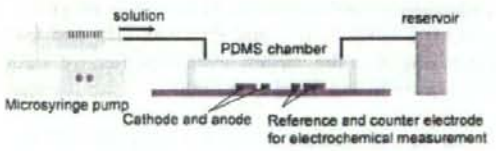

Fig. 4: Illustration of the microfluidic-type cell.

2.3 Fablication of a needle-type electrode

A prototype of needle type biofuel cell (for inserting into subcutaneous or blood vessels) was fabricated. As shown in fig. 3, in order to avoid the peel-off of an enzymatic catalyst, we tried to immobilize an enzyme within a needle. At first, a disposable injection needle (inner diameter was 0.5 mm) was insulated by electrodeposition of an insulating paint. A gold wire, which used as a current collector, was inserted in the insulated needle. Then, carbon particle and enzyme membrane were packed in order. Finally, the electrode surfaces were coated by biocompatible film.

2.4 Electrochemical measurement

The performances of the electrodes were evaluated by electrochemical measurement using three electrode systems. Except for the cyclic volutammetry shown in 3.1, all measurements were conducted using the flow-cell shown in fig. 4. Gold electrodes were patterned onto glass slide by conventional photolithography and sputtering. Anode catalysts were modified as described 2.1, and cathode catalysts were modified as reported before [7]. Flow channel (3 mm wide and 1 mm height) was made from PDMS. The flow was regulated by microsyringe pump and set to 0.3 mL min^{-1} in all measurements.

3. RESULTS AND DISSCUTTIONS

3.1 Performances of NAD-immobilized anodes

Fig. 5 shows the cyclic voltammograms (CVs) of the PLL-VK_3/PLL-NAD/Dp/GDH-immobilized anodes in a N_2-saturated phosphate buffered solution (pH 7). The peak couples around -0.3 V shows the redox activity of VK_3 on the electrode. The oxidation currents were clearly increased and reduction currents were almost disappeared in the presence of glucose, which indicated that the successful working of the polymeric NAD. Unfortunately, the catalytic activity of glucose anode was smaller than the case of dissolved NAD [4], which probably due to the low flexibility of the polymeric NAD. Utilization of longer linker would improve the flexibility of NAD [2, 4]. However, the catalytic current gradually decreased with the several time of scan, probably due to the dissolution of PLL-NAD. In order for avoid the dissolution of the PLL-NAD and improve the stability, the electrode surfaces were overcoated with bio-adoptive membranes: Nafion membrane, MPC polymer and LLC membrane. Among these three membrane-coated electrode, LLC-coated one showed the highest stability (data not shown).

Fig. 6 shows the cell performances using the LLC-coated bioanode evaluated in the microfluidic cell.

Circle plots show the cell performance using Ag|AgCl as a cathode and triangle plots show the cell performance using biriubin oxidase (BOD)-adsorbed carbon black electrode as a biocathode. The maximum current of both of two cells was about 170 μA cm^{-2}. The maximum voltage was 0.45 V higher in the glucose-O_2 cell because of the positive reaction potential of BOD cathode. The obtained maximum power densities of 80 μW cm^{-2} and 20 μW cm^{-2} were thought to be sufficient for powering the low power CMOS circuit. Therefore the cell can be used as the batteries of the low power-required electronic devices such as sensors. The time courses of the biofuel cells were plotted in fig.6 bottom. The output currents were almost stable during 6 hour operation.

3.2 Biocompatibility of electrode surfaces

Fig. 7 shows the time courses of the back ground-collected fluorescent intensity on the untreated (●), MPC-coated (▲), Nafion-coated (×) and LLC-coated (♦) bioanodes. We evaluated the biocompatibility of the electrode surface by observing the amount of adsorbed albumin, because it is the major protein in body fluids. As shown in fig. 7, the amount of albumin was gradually increased with time. LLC-coated anode showed relatively higher albumin adsorption among the four electrodes. Not only the MPC-coated electrode surface, which is well known to biologically-inert surface due to its lipid bilayer-like structure, the surfaces of the bare and Nafion-coated electrode showed lower albumin adsorption, which probably because their negatively charged surfaces electrostatically inhibited the albumin adsorption.

The relation between protein adsorption and electrode activity was evaluated. Albumin-adsorbed electrodes showed somewhat lower glucose oxidation activity except for the LLC-coated electrodes. Interestingly, the activities of LLC-coated electrodes stored in albumin solution were gradually increased with time in spite of higher protein adsorption to the surface (data not shown).

The protein blocking ability of the membrane-coated electrode surfaces is important because the protective response of our body against a foreign body starts with protein adsorption to the surface. The results obtained in fig. 7 suggested that the addition of negatively charged lipids would improve the bio-inactivity and the stability of the LLC-coated bioanode in body fluids.

3.3 The performances of needle-type electrodes

The performance of the enzyme-modified needle-type electrodes inserted in a silicone tube (1 mm in inner diameter) was shown in fig. 5. The surface of the enzyme membrane was coated with LLC and whole electrode surface was further coated with MPC polymer. An Ag|AgCl electrode was used as a cathode. The maximum voltage of the needle-type cell were slightly smaller than that obtained in 3.2 (Fig 6), which probably caused by nonuniform coatings of the enzyme membrane at needle-type miniature electrode; some area of the carbon black surface might not be covered with enzyme membrane. On the other hand, the maximum current density of a 110 μAcm^{-2} could be obtained.

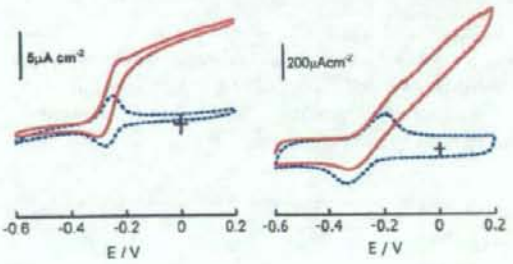

Fig. 5: CVs of the bioanode on a smooth GC electrode (left) and a CB-modified GC electrode (right) in absence of (dotted lines) and presence of (solid lines) 200 mM glucose. Scan rate was 5 mV s^{-1}.

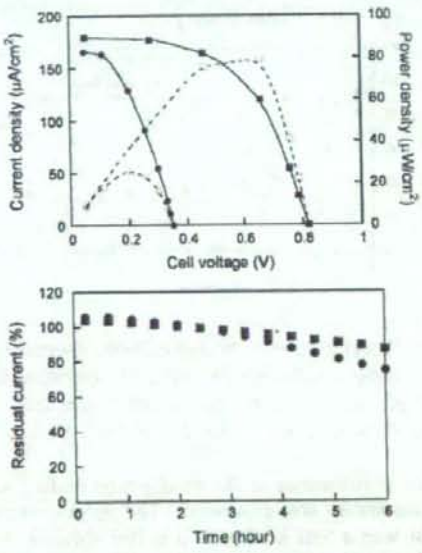

Fig. 6: Power performances (top) and stability (bottom) (R=1 MΩ) of the glucose-Ag|AgCl cell (●) and glucose-O_2 cell (■). The cells were working under 0.1 M glucose and 0.1 M NaCl-containined phosphate buffer (pH 7). Flow rate: 0.3 mL min^{-1}

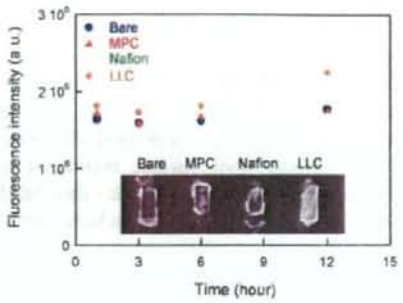

Fig. 7: Time course fluorescence intensity of the untreated (●) MPC-coated (▲) Nafion-coated (×) LLC-coated (♦) bioanode. Inset shows fluorescence micrograph of each electrode.

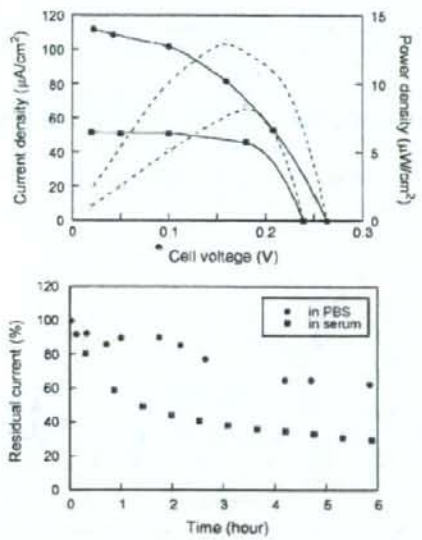

Fig. 8: Power output (top) and stability (bottom) (R = 2 MΩ) of the needle-type biofuel cells operating under 5 mM glucose-contained phosphate buffer (pH 7)(●) and bovine serum (■). Flow rate: 0.3 mL min^{-1}

The performance of the needle-type biofuel cell in a bovine serum was evaluated. The output maximum current was a half of that in a buffer solution, which also due to the uncovered carbon black electrode, so the various kinds of electroactive species might be reacted on the electrode surface. In a buffer solution, needle-type biofuel cell maintained its output current over 60 % of the initial during 6 hours of operation. The value 60 % was close to the result obtained in fig. 6. On the other hand, residual activity of biofuel cell in a bovine serum at 6 hour was smaller than that in buffer solution. Output current was rapidly decreased for first 1 hour, and then the current was almost stable, which probably due to the protein adsorption to the surface and/or degradation of the LLC-membrane was caused at early stage. Uniform coatings of enzyme catalysts and development of a stable overcoat membrane would improve the stability of needle-type biofuel cell.

4. CONCLUSION

The prototype miniature biofuel cells composed of needle-type electrode immobilized with organic and harmless electrocatalysts produced ca. 110 μA cm^{-2} of current density and maintain the current over 60 % of the initial during 6 hours of operation. To stabilize the power output in serum, bioinert coating, fabrication method and structure of miniature electrode should be optimized. Future work will also be focused in making a miniature polymer-needle array by microfabrication techniques for developing the painless and easily disposable implantable miniature biofuel cell.

REFERENCES

[1] Barton S C, Gallaway J and Atanassov P 2004 Enzymatic biofuel cells for implantable and microscale devices *Chem. Rev.* **104** 4867-86.

[2] Heller A 2004 Miniature biofuel cells *Phys. Chem. Chem. Phys.* **6** 209-16.

[3] Kamitaka Y, Tsujimura S, Setoyama N, Kajino T and Kano K 2007 Fructose/dioxygen biofuel cell based on direct electron transfer-type bioelectrocatalysis *Phys. Chem. Chem. Phys.* **9** 1793-801.

[4] Togo M, Takamura A, Asai T, Kaji H and Nishizawa M 2007 An enzyme-based microfluidic biofuel cell using vitamin K_3-mediated glucose oxidation *Electrochim. Acta* **52** 4669-74.

[5] Sato F, Togo M, Islam M K, Matsue T, Kosuge J, Fukasaku N, Kurosawa S and Nishizawa M 2005 Enzyme-based glucose fuel cell using Vitamin K_3-immobilized polymer as an electron mediator *Electrochem. Commun.* **7** 643-7.

[6] Rowinski P, Kang C, Shin H and Heller A 2007 Mechanical and chemical protection of a wired enzyme oxygen cathode by a cubic phase lyotropic liquid crystal *Anal. Chem.* **79** 1173-80.

[7] Togo M, Takamura A, Asai T, Kaji H and Nishizawa M 2008 Structural studies of enzyme-based microfluidic biofuel cells *J. Power Sources* **178** 53-8.

MINIATURED BIOFUEL CELLS AUTOMATICALLY RELAYED FOR LONGER-TERM POWER GENERATION

Masato Oike, Makoto Togo, Hirokazu Kaji, Takashi Abe and Matsuhiko Nishizawa
Department of Bioengineering and Robotics, Graduate School of Engineering, Tohoku University

Abstract: The present study reports a new stepwise power generation system for prolonging total lifetime of miniature biofuel cells. This system consists of parallelly-connected electrodes that were designed to be automatically activated at different timing after exposure to fuel solution by using a magnetic plastic cover and degradable glue. The timing of activaiton could be controlled by adjusting the weight ratio of Fe_3O_4 in the covers and the kind of degradable glues. The stepwisely increased power output of this system was eventually higher than the ordinary system.

Key words: biofuel cell

1. INTRODUCTION

Biofuel cells are promising for miniature power sources because of their specific characters such as high reaction selectivity and organic-based components, which enables to construct renewable, miniature and safe systems. In addition, biofuel cells are able to generate electricity from complex solution containing fuel and oxidant such as soft-drink, alcohol and blood. Despite these merits, there are some problems to be solved. The problematic lower power has recently been improved rapidly by using nano-materials as electrode. Another remaining problem is stability of the cell. The lifetime of an enzymatic biofuel cell is usually determined by enzyme stability which could be improved by protein engineering and immobilized state of enzymes. In recent days, some researchers suggested that the immobilized enzymes within a microstructure, such as a meso-porous carbon matrix [1] or Nafion membrane [2], showed higher stability.

We report here an attempt for prolonging total lifetime of miniature biofuel cells. Fig. 1 (a) shows the principle of our system, in which micro-biofuel cells protected with different kinds of degradable films are arrayed and connected in parallel. Each of the cells is designed to be activated at different time intervals after exposure to the fuel solution. The timing of activation will be controlled by the properties of the degradable films: the material used, molecular weight, composition, or thickness. Then, the total power output can be expected to be more stable than an ordinary system (Fig. 1 (b)).

We have demonstrated that the provisional protection of subsets of biofuel cells was effective in prolonging the total lifetime of the fuel cell system [3]. In the primary experiments, we fabricated the devices like fig. 1 with 70 μm-thick poly(lactic-co-glycolic acid) (PLGA) films as degradable protect membranes. After exposing to solution, PLGA cover films were swollen, lost its rigidity and attached to electrodes before the membranes were dissolved away. When the electrodes were wet with swollen membrane, the cell started generating electricity. Consequently it was difficult to control the exposure time of the stored electrode. Therefore, in this paper we used degradable materials as just glue not as the protect membrane itself. In addition, we thought that some additional forces might be required to peel off the protection

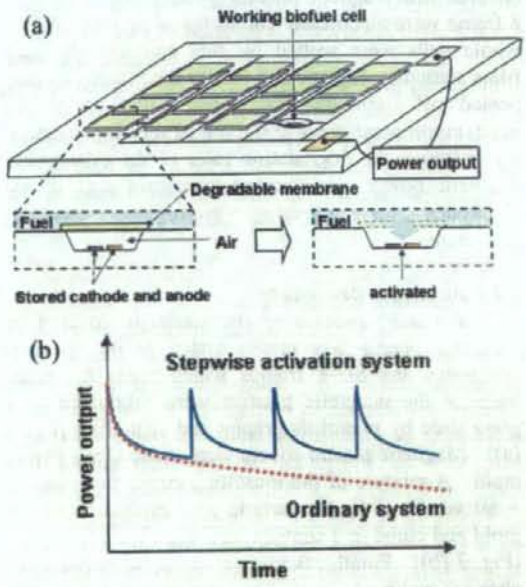

Fig. 1: (a) Schematic illustration of an array of miniature biofuel cells protected with degradable films that can be stepwisely degraded. (b) The image of the expected performance of the stepwise activation system.

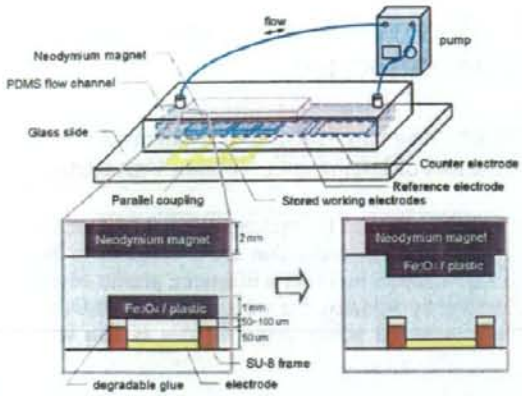

Fig. 2: Prototype of miniature biofuel cells.

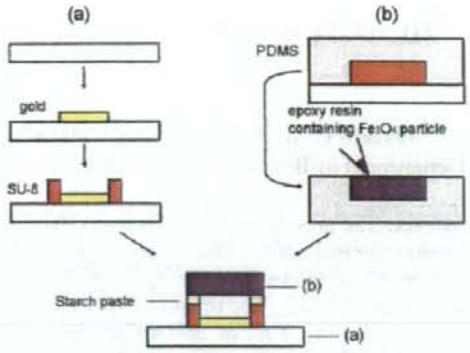

Fig. 3: Fabrication process of (a) electrode and SU-8 frame patterned on a glass slide, (b) magnetic plastic cover and their lamination.

membranes. As shown in fig. 2, we applied magnetic force to lift up the membrane from the electrodes area.

2. EXPERIMENTAL

2.1 Construction of the biofuel cell

We designed and tested a degradable device to investigate the feasibility of multi-pulse electrode activation without any external trigger. Fig. 2 shows the experimental system in this study. Electrodes covered with magnetic plastics which glued to the SU-8 frame were electrically connected in parallel. When whole cells were wetted by fuel solution, the glue films started to degrade and finally the magnetic cover peeled off from the frame and lifted up to the neodymium magnet set at the top of the flow channel. By changing the degradation rates of the glue and/or magnetic power, we adjusted the stored time of the electrodes for achieving multi-pulse electrode activation.

2.2 Fabrication procedure

Fabrication process of the electrode covered by magnetic plastic was briefly stated in fig. 3. Gold electrodes and SU-8 frames which made for being basis of the magnetic plastics were fabricated on a glass slide by photolithography and spattering (Fig. 3 (a)). Magnetic plastic covers were made using PDMS mold. A mixture of thermosetting epoxy resin and 10 ~ 60 wt. % of Fe_3O_4 particle was applied to PDMS mold and cured in a conventional oven for a few hours (Fig. 3 (b)). Finally, these two components described above were glued together by using starch paste which is common water-soluble glue. Here, the starch paste was stenciled on the magnetic cover so as to be ca. 100 μm-thick.

A 5 mm-height and 6 mm-wide PDMS flow channel was fabricated. As shown in fig. 2, a 2 mm-thick neodymium magnet plate was set at the roof of the flow channel. Glass layer and PDMS flow channel were laminated, and connected to peristaltic pump through silicone tube.

2.3 Preparation of electrocatalysts

When using an enzyme electrode as a working electrode, gold electrode was modified with carbon particle, electron mediator polymer and enzymes [4, 5]. A brief description of the preparation follows. An 8 μL PLL-VK_3 solution (4.83 mM VK_3) was mixed with a 2 μL Dp solution (14 μg μL^{-1}) and 1 μL of KB dispersed water (ca. 13 mg mL^{-1}). A 1.5 μL portion of the resulting solution was put onto a gold film electrode (surface area, 0.0225 cm^2) on a glass substrate, and was left to dry in air. To create the enzymatic bilayer, the surface of a PLL-VK_3/Dp-coated KB electrode was coated with 1.4 μL of a solution composed of equal volumes of a 16 μg μL^{-1} GDH solution and a 16 mg mL^{-1} PLL solution.

2.4 Electrochemical measurement

All electrochemical measurements were performed in 50 mM phosphate buffer solution (pH 7.0) containing 0.1 M NaCl at room temperature. The electrochemical output of the electrodes were collected using an Electrochemical Analyzer (Model 600S, BAS) with three electrode system containing an enzyme-modified electrode as the working electrode, an Ag|AgCl (0.1 M NaCl) reference electrode and a gold counter electrode. All measurements were conducted using constant voltage mode. A peristaltic pump (SJ-1220-2, ATTO) was used to make a controlled flow in the fluidic channel.

3. RESULTS AND DISSCUTTIONS

3.1 Parameters affecting storage time

We studied the effects of Fe_3O_4-contens in plastic cover and flow conditions on the time-delay for exposure of electrodes (storage time) by measuring the oxidation current of $Fe(CN)_6$. Fig. 4 shows the typical result of the stepwise electrode activation using the system described in 2.1. During the electrode was covered with the magnetic plastic, the observed current was nearly zero, and then the current was rapidly increased with lifting up of the magnetic plastic cover when the glue was degraded (gradually swelled and dissolved) and adhesion force was getting weaker than magnetic force (Fig. 4 (a)). In the following experiments, the exposure of the electrodes was judged from the electrical pulse like shown in fig. 4 (b).

At first, we found that the drying time of the starch paste was affected to the storage time of the electrode. Shorter drying time made the storage time shorter probably due to the residual water in a starch paste which will affect the adhesion force and its stability. These results indicate that the material property of the glue could control the storage time of the electrodes. The storage times of the electrodes were almost constant over 12 h of drying. In the following experiments, the drying time of the starch glue was set to around 24 h.

As shown in fig. 5 (a), the storage times were shorter when the used plastic covers contained larger amount of Fe_3O_4. Unfortunately averaged storage times of 40 and 20 wt. % Fe_3O_4-contained magnetic plastics did not show clear difference in the storage time. The data variation is thought to be causally related to unevenness of the starch glue coated on the magnet plastic. In fact, the viscosity of starch paste was too high to be coated thinly and evenly.

Fig. 5 (b) shows the relation between storage times and flow rates. Storage time at each flow velocity was around 0.2 hours. These results indicate that the degradation rate of the starch paste was not related to the flow velocity at least in this range. And the results also suggest that the flow direction and/or electrode arrangement might not be related to the degradation rate of the glue.

3.2 Stepwise electric power generation

Fig. 6 shows the time course of the output current from the prototype device shown in fig. 2. The device had parallelly-connected four enzyme electrodes which prepared as described in 2.3. Each electrode was covered with the magnetic plastic containing 60, 40, 20, and 10 wt. % Fe_3O_4 particle and glued with degradable starch paste (Fig. 6 (b)). We also prepared uncovered parallelly-connected four enzyme

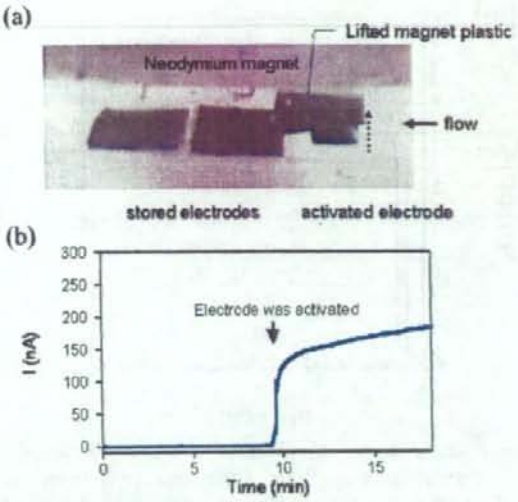

Fig. 4: Typical photograph and time course of current produced by the prototype device covered with the magnetic plastic.

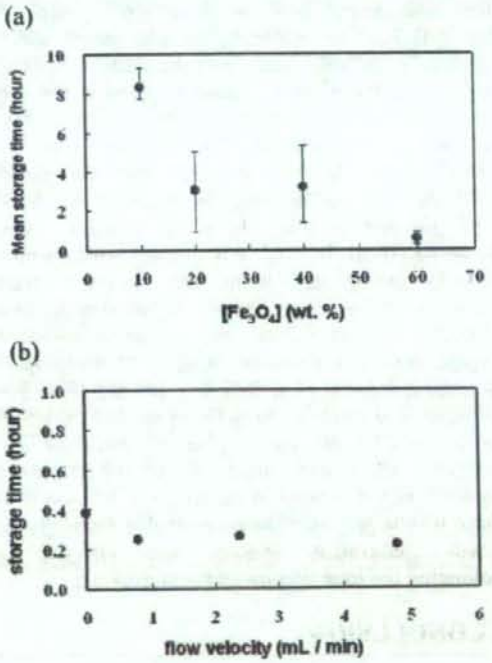

Fig. 5: Parameters affecting to storage time of electrodes (a) the mixture ratio of Fe_3O_4, (b) the flow rate. The measurements were performed three times in the phosphate buffer (pH 7) containing 5 mM $K_3[Fe(CN)_6]$, 0.1 M NaCl, at room temperature, with a flow rate of 0.8 mL min^{-1} (a).

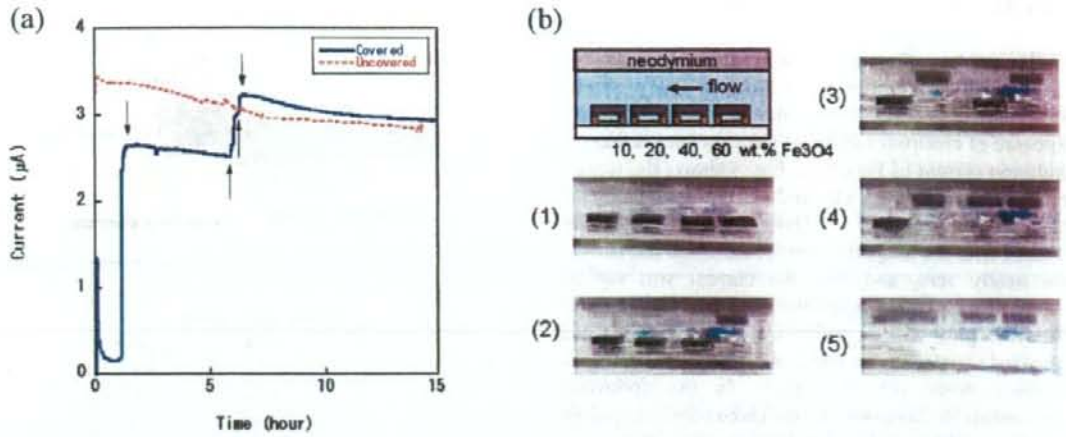

Fig. 6: Time course of (a) the current and (b) typical photographs produced by prototype of miniature biofuel cells covered with magnetic plastic and starch paste. The cell was working under 50 mM glucose, 5 mM NAD^+ and 0.1 M NaCl containing phosphate buffer solution (pH 7). The flow rate was 0.8 mL min^{-1}.

electrodes as the control. By using enzyme electrodes as anodes and Ag|AgCl electrode as a cathode, the output current of the glucose biofuel cell (R = 100 kohm) was measured in an air-saturated phosphate buffer (pH 7, 37°C) containing 50 mM glucose and 5 mM NAD^+. The solid line shows the output current of electrodes covered with magnetic plastics and the dotted line shows the current of uncovered electrodes. The observed small current of the covered cell at first stage (0 to 67 min) was produced from uninsulated lead wires. The current suddenly increased to 2.6 μA at 67 min due to lifting up of the magnetic cover containing 60 wt. % Fe_3O_4 (Fig. 6 (b)-(2)) and then the electrode was activated. In this term, the power output of uncovered electrodes was still higher than covered electrodes. Around 6 hours later, the power output of covered electrodes increased rapidly with lifting up of the magnetic cover (Fig. 6 (b)-(3), (4) and (5)). The difficulty in controlling the storage time was caused by the unevenness of starch glue as described 3.1. However, the power output of covered electrodes exceeded that of uncovered electrodes at 360 min (6 h). These results principly demonstrate that the stepwise power generation system was effective in prolonging the total lifetime of the biofuel cell.

4. CONCLUSION

We demonstrated that the provisional protection of subsets of biofuel cells is effective in prolonging the total lifetime of the fuel cell system. In this experiment, we obtained several hours of electrical pulse interval by using the magnetic cover glued with starch paste. Practically, much longer interval or precise control of the storage time should be obtained. In such case, PLGA glue is hopeful because the PLGA glue could store the electrode for a few days or more in other preparatory experiment. In addition, future work will be focused on replacing the magnet power to another power such as buoyancy of cover materials.

REFERENCES

[1] Tsujimura S, Kamitaka Y, Kano K 2007 Diffusion-controlled oxygen reduction on multi-copper oxidase-adsorbed carbon aerogel electrodes without mediator *Fuel Cells* **7** 463-469

[2] Moore C M, Akers N L, Hill A D, Johnson Z C, Minteer S D 2005 Improving the environment for immobilized dehydrogenase enzymes by modifying Nafion with tetraalkylammonium bromides *Biomacromlecules* **5** 1241-1247

[3] Asai T, Togo M, Oike M, Morimoto K, Kaji H, Abe T, Nishizawa M 2007 Biofuel cells using biodegradable plastic *Abstract paper for the annual meeting of ECSJ (Tokyo, Japan, 19-20 September 2007)*

[4] Togo M, Takamura A, Asai T, Kaji H, Nishizawa M 2008 Structural studies of enzyme-based microfluidic biofuel cells *J. Power Source* **178** 53-58

[5] Togo M, Takamura A, Asai T, Kaji H, Nishizawa M 2007 An enzyme-based microfluidic biofuel cell using Vitamin K_3-mediated glucose oxidation *Electrochim. Acta* **52** 4669-4674

3 バイオ燃料電池マイクロシステムと体液発電への取り組み

西澤 松彦

1 はじめに

電子機器の超小型化・省電力化に呼応して，身の回りに分散する低密度エネルギーを有効利用するエネルギーハーベスティング技術の開発が盛んであり，バイオマイクロ燃料電池の研究動向にも注目が集まっている[1-3]．生体触媒（酵素）を利用するバイオ電池は，出力性能や寿命に課題を有しつつも，圧倒的に安全で使い捨て利用も可能な，環境・生体親和性に優れる発電デバイスとして期待されている．これらの利点と弱点を十分に意識した応用分野の設定と，対応するデバイス設計，および作製プロセス技術の開発を推し進めることが，他の発電システムとの差別化と将来の実用化に向けて重要といえる．

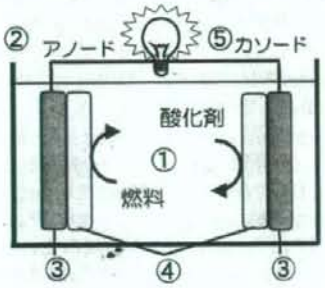

① 燃料や酸化剤の供給，効率的利用
→ 層流，マイクロポンプ
② 実装，配線，積層アレイ化
直列電池間の絶縁
→ マイクロバルブ
③ 電極，多孔質電極
④ 酵素，メディエーターのパターニング
⑤ 制御回路(LSI)，センサ，
アクチュエータ等との一体化

Fig. 1 バイオ燃料電池システムへの活用が期待されるMEMS製造技術．

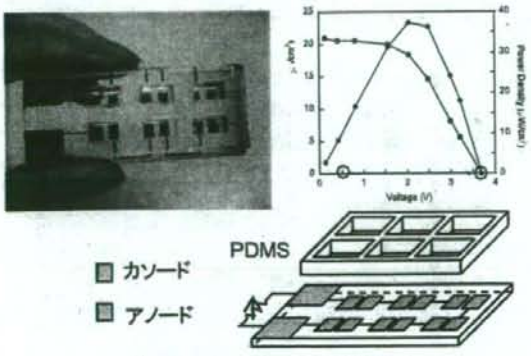

Fig. 2 パッチ式バイオ電池アレイ．

バイオ燃料電池を小型システムとして構成するのに力を発揮するのがMEMS（Micro Electro Mechanical Systems）技術である．ノート型パソコンなどへの搭載が検討されるマイクロDMFC（直接メタノール型燃料電池）[2]と同様に，バイオマイクロ燃料電池もPowerMEMSの一種として発展していくと思われる．その際，有機電子デバイスであるバイオ燃料電池に対応して，ポリマーの微細加工などにおいてMEMS技術自体が進展するだろう．本稿の前半では，微細加工によってバイオ燃料電池の特長を活かし，弱点を補おうとする取り組みを紹介する．

一方，小型で安全なバイオマイクロ燃料電池のメリットがストレートに活きる応用領域のひとつは医療，特に体内埋め込み電源としての利用であり，体液からの発電である．本稿の後半では，医療分野への適用を目指した研究・技術開発の動向について述べたい．

2 MEMS技術によるバイオ燃料電池の小型化・機能化

バイオ燃料電池にMEMS技術を積極的に取り入れた研究は未だ多くないが，Fig. 1に示すように，バイオ燃料電池の構成要素との対応は多岐にわたり重要である．燃料や酸化剤の制御には，マイクロバルブやマイクロポンプが必要となるが，既存のMEMS素子は電力を要するし使い捨てに向くとも言い難い．これまでMEMSの主要材料ではなかったポリマーなどへの技術拡張によって，バイオ燃料電池の特徴や事情に対応する必要がある．たとえば，電力を要しない高分子ゲルを利用したポンプなどもある．以下では，スタッキング（直列つなぎ）や寿命対策に関わる我々の取り組みを紹介する．

2.1 オンチップ配列による出力電圧向上の試み

バイオ燃料電池単セルの出力電圧は1 V以下であり，他の燃料電池と同様に，実用の際には積層して出力電圧を稼ぐ必要がある．しかしながら，ジュースや体液など「イオン伝導性を有する燃料溶液」を用いるバイオ燃料電池では，スタッキングが比較的難しい．乾電池の直列つなぎの要領で用いるのが常套手段であり，Fig. 2は極めてシンプルな1例である．ここで，アノード反応はビタミンK_3ポリマーをメディエータとする酵素修飾電極によるグルコースの酸化，カソード反応はPDMSディスパージョンで被覆したPtでの酸素還元である[4-6]．電極修飾膜はスクリーンプリントで一括成膜し，シリコーンポリマーの構造体でセル間を絶縁してバイオ電池をアレイ化した．設計どおり6倍の回路電圧が得られる．し

かし，燃料溶液はピペットで各セルに注入され，燃料溶液の交換もセル個々に行う必要があり，明らかに実用的でない．とはいっても，単一流路内に複数の電池を並べて燃料注入・交換を一括で行おうとしても，イオン伝導性の燃料溶液によってセル間がショートしてしまう．つまり，電池間を電気的に絶縁するためのマイクロバルブを搭載する必要がある．

マイクロ流路内に配列したバイオ電池の直列つなぎに必要なマイクロバルブとして，「安価・使い捨て・有機物で構成」などの特徴を損なわず，しかも電力を使わないという条件の下，超撥水性エアバルブを検討したのがFig. 3である．ポイントは，流路内に配列した電池の間に超撥水性の部分を造り込むことであり，そこに外部から浸入する気泡によって自動的に絶縁されるしくみでスタッキング（直列つなぎ）しようという試みである．反応性イオンエッチングで作製した鋳型の形状をポリマー材料に転写して，蓮の葉の表面形状を真似た凸凹（マイクロピラーアレイ）による超撥水性（接触角＞150°）を発現させた．ピラーの太さと間隔を変えて撥水性を系統的に評価し，太さ・間隔共に15 μmで安定な超撥水性が得られると分かった．Fig. 3bは3組の酵素電池が配列した流路に燃料溶液を注入した際の回路電圧の推移である．ここで，アノード・カソードは共にOsポリマーと酵素の混合膜である[7]．電池出力は，燃料注入の間は単セルの回路電圧0.4 V程度であるが，流れを止めると，エアバルブが働き1 Vを超える電圧が出た．

ここで開発したマイクロ流路内の液体分離技術は，オンチップバイオ計測システムにおいても重要な役割を有し，たとえば，チップ上でのマルチ呈色アッセイを可能とする技術でもある．

2．2　オンチップ配列による長期発電に向けた試み

バイオ燃料電池の出力電流は，カーボン微粒子やカーボンチューブなどのナノマテリアルによる電極表面構造の最適化などによって着実に大きくなっており，mAレベルの出力は特別ではなくなってきている[8]．出力電圧についても，MEMS技術等によるスタッキングで実用電圧への増大がはかられる．もとより，バイオ電池への期待は出力特性だけではなく，突出した安全性と，安価・小型化にあり，その背景には電子デバイスの省電力・ユビキタス化がある．むしろ，バイオ電池の応用形態を規定する重要なファクターは「耐久性（寿命）」であろう．電池性能の劣化には，電極修飾物の漏出や酵素の失活などの複数要因が関わっており，また，劣化の速度が実験条件に大きく依存するので一概には言えないが，一般に，数週間も発電を続けると大きく性能が落ちる．

耐久性改善への取り組みは，バイオ電池開発の中心的な課題として盛んに行われてきた．遺伝子工学による酵素の安定性に成果が上がる一方[9]，酵素の固定方法の改良で酵素活性を相当長期に渡って維持できたとするMinteerグループの研究報告が注目されている[10]．Nafionのチャンネル内環境を四級アンモニウム塩の配位で制御して酵素固定に用いると，1ヶ月以上活性を保持して発電できるらしい．

さて，我々は，酵素電極の劣化を前提とし，それを補うバイオ電池システムの構造をMEMS工学の視点から探っている．現在，Fig. 4に示すように，複数のアレイ化した電池が時差を有して順々に発電を開始するしくみを，生分解性高分子などのマイクロ加工で創出しようと試みている．例えば，乳酸とグリコール酸の共重合体（PLGA）の分解速度は，モノマー比によって数時間～数ヶ月の間で制御できる．これで並列に配置したバイオ電池カバーしておき，順々に活性化と

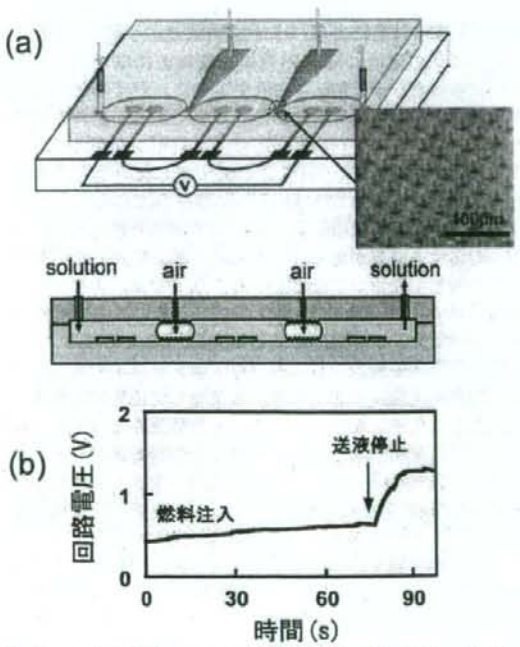

Fig. 3　(a) 半自動エアバルブによる流路内直列スタッキング
(b) 得られた回路電圧の一例．

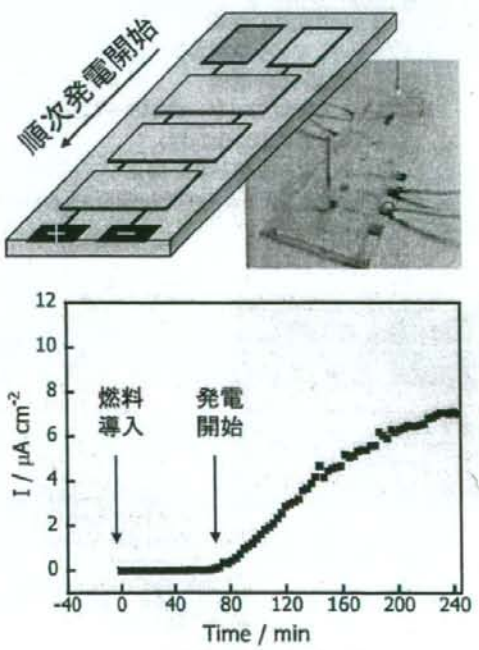

Fig. 4　時差式発電への取り組み．

発電が始まる時差式発電の機構が実現すれば，「長寿命」なバイオ発電システムができるかもしれない．研究のポイントは，酵素電極の活性を損なわないPLGAの接合技術である．加圧CO_2（37℃, 0.7 MPa）によるPLGA接合を利用したが[11]，これはタンパク質の活性に全く影響を与えない，極めてマイルドな方法であり，バイオMEMS全般の作製に幅広く貢献し得る．このようなバイオ材料にも使える加工・接合技術の開発を，バイオ電池の研究を通じて模索したいと考えている．

3　メディカル応用と体内発電

3．1　体内埋め込み電子デバイスの電源事情

バイオマイクロ燃料電池にとって，メディカル応用，特に体内埋め込み電源としての利用は，古くからその実現が待望される，重大な使命である．ペースメーカーや人工内耳，神経刺激によるパーキンソン病や心不全の治療，鎮痛や化学療法のための薬剤投与デバイス，人工眼の開発など，既に実用化しているものから，未だ緒についたばかりのものまで，多様な埋め込み型医療デバイスの開発研究がQOL向上を目指して加速している[12,13]．これら医療デバイスのいずれにおいても，電力の供給は重要な課題であり，電源のサイズや性能がデバイス全体の形状や応用形態を左右するケースが少なくない[12,13]．ペースメーカーには20年来リチウムーよう素電池が用いられており，数μAの電流パルスを10年以上安定に発生する信頼性を得ている[13]．mAレベルの電流を要する他のデバイスへは，カップリングコイルの誘導起電力を利用し，外部から高周波で電力供給する技術が盛んに検討されている[12]．体温で発電するバイオサーマル電池の検討も行われている．バイオマイクロ燃料電池は，これら電源システムのオプションのひとつであり，血液や組織液に含まれるグルコースと溶存酸素で発電する．

体液発電の実績の多くは，酵素ではなく白金などを電極触媒とする燃料電池で得られており[14]，既に60年代には人工心臓の開発の一環として研究が始まり，70年代には動物を使った*in-vivo*実験も盛んに行われ，犬の体内で数μW/cm²を数ヶ月間に渡って出力できている[15]．触媒の反応選択性が低いので，Fig. 5に示すような構造がとられる．燃料溶液（体液）に接したカソードで酸素が消費され，グルコースのみがアノードに到達する構造である．活性炭を酸素選択性のカソードに用いたタイプが盛んに検討された．しかしながら，当時の目的であった人工心臓の駆動には出力が足りず，研究の停止期間があったが，低消費電力のMEMS埋め込みデバイスの登場で再注目されている[14]．たとえば，最近の，フライブルグ大学F. von Stettenらの報告では[16]，出力は依然としてμW/cm²レベルで低いけれども，1ヶ月以上の連続発電でも性能の低下がほとんど認められない長期安定性が実証されている．埋め込みデバイスの表面に貼り付けて一体化できる形状でもあり（2 cm²），実用化への期待が大きい．

3．2　酵素燃料電池による体液発電への取り組み

酵素を使うバイオ燃料電池の特徴は，酵素触媒の優れた反応選択性にある．それゆえ，Fig. 5で述べたような特殊構造が不要で，セパレーターも要らない．Fig. 6は，グルコース酸化用の酵素アノードと，PDMSディスパージョンを塗布してO_2選択性を付与したPtカソードによる発電実験[4-6]の例で，コーヒーや血清からも同じように発電できている（カーボン粒子などを使ってないので出力小さい）．すなわち燃料溶液の精製が必要ない．カソードの酸素還元反応もBODなどの酵素で触媒できる．Texas のHeller博士のグループは，古くから体液発電を指向しており，針状の微小なバイオセンサへ搭載して実用化を目指している[17,18]．

Fig. 6の中で血液を用いた際の結果は，血清の場合に比べて大きく劣っている．測定後に電極表面を観察するとゼリー状の付着物に覆われていた．これは，いわゆる血栓様のバイオ付着であり，これが物理的・化学的に電極反応を阻害すると思われる．血栓形成は，不溶性フィブリンの生成，血小板凝集，補体系による白血球粘着，という3通りのシステムがタンパク質の吸着によって誘起された結果と考えられている．

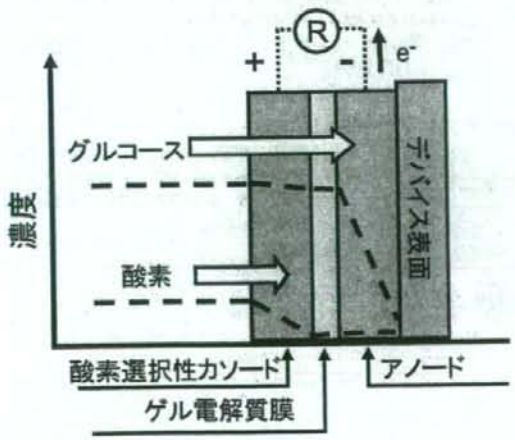

Fig. 5　酵素を使わない体液発電デバイスの構造（参考文献14から改変）．

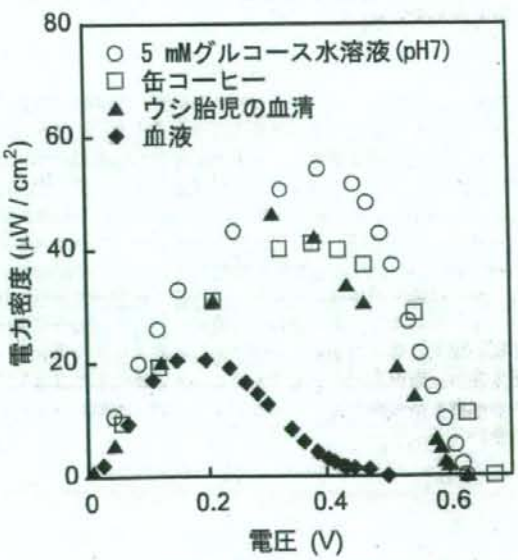

Fig. 6　グルコース水溶液，缶コーヒー，ウシ血清，筆者の血液からの発電実験．

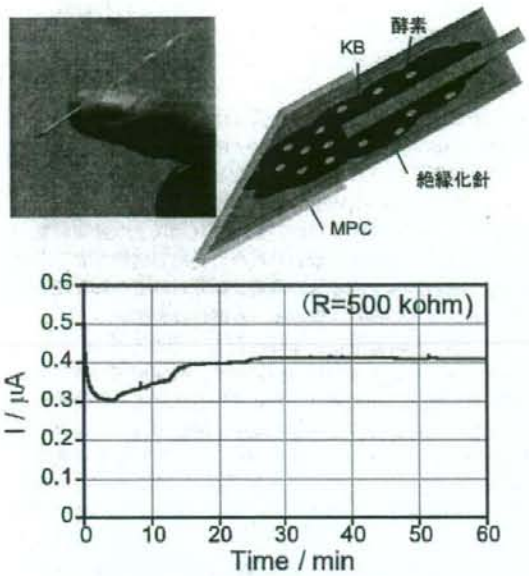

Fig. 7　針状酵素電極と発電実験.

タンパク質の吸着を防ぐために，ポリエチレンオキシド（PEO）のグラフト化，ヘパリンやアルブミンといった抗血栓性生理活性分子の固定化，2-メタクリロイルオキシエチルホスホリルコリン（MPC）ポリマーの塗布による生体膜類似構造の形成，などが有効とされている[19]．Fig. 7の針状バイオ電池の先端もMPCポリマーでバイオ付着を防いである．適切な被覆を行うと，電極反応（物質移動）の妨げにならずに抗血栓性が認められる．ゴムチューブに針状のアノード・カソード刺して，5 mM GlucoseのPBS溶液から安定に電流を取り出している．

4　おわりに

酵素を電極触媒とするバイオ燃料電池は，小型化が容易で非常に安全な発電デバイスであり，小型電子デバイスや未来医療デバイスを支援するユビキタス電源として見逃せない位置づけにある．ここでは，バイオ燃料電池の小型化と機能化に有効なMEMS技術を，今後の主流である高分子材料の加工を例にとって解説した．また後半では，メディカル応用について述べた．μTASとしての検査チップから，経皮的なもの，皮下組織への埋植，血管への埋め込みなど，多様なバリエーションが有り，その侵襲性の程度によって実用の可能性や検討課題は様々である．体内深部への埋め込みを考えると，耐久性の一層の向上が必要であるし，抗血栓性や生体適合性への配慮も不可避となり，その実現に向けて克服すべき問題は多い．

謝　辞

本稿では，厚生労働省科研費「分散型ナノ植え込み機器を活用した慢性心不全患者の統合的デバイス治療の開発」のご支援の下，博士研究員の都甲真による成果を紹介しました．感謝します．

文　献

1) バイオ電池の現状と展望，エコインダストリー，CMC出版（2005）.
2) 電池革新が拓く次世代電源，エヌ・ティー・エス（2006）.
3) バイオ電気化学の実際，CMC出版（2007）.
4) F. Sato, M. Togo, M. Islam, T. Matsue, J. Kosuge, N. Fukasaku, S. Kurosawa, and M. Nishizawa, *Electrochem. Commun.* **7**, 643 (2005).
5) M. Togo, A. Takamura, T. Asai, H. Kaji, and M. Nishizawa, *Electrochim. Acta*, **52**, 4669 (2007).
6) M. Togo, A. Takamura, T. Asai, H. Kaji, and M. Nishizawa, *J. Power Sources*, **178**, 53 (2008).
7) S. Tsujimura, K. Kano, and T. Ikeda, *Electrochemistry*, **70**, 940 (2002).
8) Abstract of 213th ECS meeting (2008).
9) N. Yuhashi, M. Tomiyama, J. Okuda, S. Igarashi, K. Ikebukuro, and K. Sode, *Biosens. Bioelectr.*, **20**, 2145 (2005).
10) M. J. Moehlenbrock and S. D. Minteer, *Chem. Soc. Rev.*, **37**, 1188 (2008).
11) Y. Yang, Y. Xie, X. Kang, L. J. Lee, and A. Kniss, *J. Am. Chem. Soc.*, **128**, 14040 (2006).
12) Special Issue: The Bionic Human, *Science*, **295**, 995, (2002).
13) G. Pistoia, Batteries for Portable Devoces, Elsevier, Chapter 6, 2004.
14) S. Kerzenmacher, J. Ducree, R. Zengerle, and F. von Stetten, *J. Power Sources* (2008), doi: 10.1016/ j. jpowersour. 2008. 03. 031.
15) E. Weidlich, G. Richter, F. von Sturm, and J. R. Rao, *Biomatr. Med. Devices Artif. Organs* **4**, 277 (1976).
16) S. Kerzenmacher, R. Sumbharaju, J. ducree, R. Zengerle, F. von Stetten, Transducers '07-Digest of Technical Papers, Lyon, France, 2007, 125.
17) A. Heller, *Phys. Chem. Chem.* Phys., **6**, 209, 2004.
18) A. Heller, *AIChE J.*, **51**, 1054, 2005.
19) 石原一彦ほか，バイオマテリアルサイエンス，東京化学同人，p.117, 2003

●著者プロフィール

氏名：西澤　松彦　Matsuhiko NISHIZAWA
所属：東北大学工学研究科バイオロボティクス専攻（〒980-8579　仙台市青葉区荒巻字青葉6-6-01）
役職：教授
趣味：ゴルフ少々